Monitoring MR-guided High Intensity Focused Ultrasound therapy using transient Supersonic Shear Wave MR-Elastography

Ounay Ishak, Élodie Breton, Karine Choquet, Anne Josset, Paolo Cabras, Jonathan Vappou

Physics in Medicine & Biology

IPEM Institute of Physics and Engineering in Medicine

ACCEPTED MANUSCRIPT

Monitoring MR-guided high intensity focused ultrasound therapy using transient supersonic shear wave MR-elastography

To cite this article before publication: Ounay Ishak *et al* 2022 *Phys. Med. Biol.* in press https://doi.org/10.1088/1361-6560/acac5e

Monitoring MR-guided High Intensity Focused Ultrasound therapy using transient Supersonic Shear Wave MR-Elastography

Authors

Ounay Ishak[1], Elodie Breton[1], Karine Choquet[1], Anne Josset[1], Paolo Cabras[1,2] and Jonathan Vappou[1]

[1]*Université de Strasbourg, CNRS, ICube, UMR7357, Strasbourg, France*
[2]*Image Guided Therapy, Pessac, France*

Abstract

Objective

The aim of the paper is to propose an all-in-one method based on Magnetic Resonance-Supersonic Shear wave Imaging (MR-SSI) and Proton Resonance Frequency Shift (PRFS) to monitor High Intensity Focused Ultrasound (HIFU) thermal ablations.

Approach

Mechanical properties have been shown to be related to tissue damage induced by thermal ablations. Monitoring elasticity in addition to temperature changes may help in ensuring the efficacy and the accuracy of HIFU therapies. For this purpose, an MR-SSI method has been developed where the ultrasonic transducer is used for both mechanical wave generation and thermal ablation. Transient quasi-planar shear waves are generated using the acoustic radiation force, and their propagation is monitored in motion-sensitized phase MR images. Using a single-shot gradient-echo echo-planar-imaging (EPI) sequence, MR images can be acquired at a

sufficiently high temporal resolution to provide an update of PRFS thermometry and MR-SSI elastography maps in real time.

Main results

The proposed method was first validated on a calibrated elasticity phantom, in which both the possibility to detect inclusions with different stiffnesses and repeatability were demonstrated. The standard deviation between the 8 performed measurements was 2% on the background of the phantom and 11%, at most, on the inclusions. A second experiment consisted in performing a HIFU heating in a gelatin phantom. The temperature increase was estimated at 9 °C and the shear modulus was found to decrease from 2.9 to 1.8 kPa, reflecting the gel softening around the HIFU focus, whereas it remained steady in non-heated areas.

Significance

The proposed MR-SSI technique allows monitoring HIFU ablations using thermometry and elastography simultaneously, without the need for an additional external exciter as those used in MR Elastography.

Keywords: MR Elastography, Supersonic shear wave, Thermal ablation, HIFU therapy, Therapy monitoring, Interventional MRI

Introduction

High Intensity Focused Ultrasound (HIFU) is a non-invasive, non-ionizing thermal ablation method that has shown great potential for cancer treatment, when combined with appropriate and accurate monitoring methods (Geoghegan *et al* 2022). To date, Magnetic Resonance Thermometry (MRT) is considered as the gold standard for non-invasive monitoring of temperature changes during thermal ablations. Proton Resonance Frequency Shift (PRFS) MRT is a relatively tissue-independent temperature estimation method, with the exception of adipose tissue (Ishihara *et al* 1995, Quesson *et al* 2000, Rieke and Butts Pauly 2008). In practice, temperature is used as an instantaneous biomarker of the ablation, but this information does not directly inform the physician about the structural integrity of the tissue (Odéen and Parker 2019). In theory, thermal dose can provide such information (Sapareto and Dewey 1984), but it has the drawback of being highly sensitive to noise since it relies on the integration of temperature over time. Therefore, systematic errors on temperature will also be integrated in time and thus, may lead to amplified errors on thermal dose estimates. Therefore, complementary biomarkers are needed to ensure permanent feedback on the state of the tissue during and after ablation.

It has been shown that mechanical properties are sensitive to tissue damage caused by heating and thus, can be used as a complementary biomarker for HIFU monitoring (Arnal *et al* 2011, Sapin-de Brosses *et al* 2010, Corbin *et al* 2016, Chen *et al* 2014, Mariani *et al* 2014, E. Konofagou *et al* 2012). Elastography monitoring methods were first introduced in ultrasound imaging to assess tissue damage during thermal ablations (Arnal *et al* 2011, Mariani *et al* 2014). Magnetic Resonance Elastography (MRE), initially used for diagnostic purposes (Lewa 1991, Muthupillai *et al* 1996), has also been shown to be applicable for monitoring thermal ablations. MRE has been used for assessing elasticity changes before and after the procedure (Chen *et al* 2014, Wu *et al*

2001), as well as during the ablation in real time (Corbin *et al* 2016, Yuan *et al* 2007). Nonetheless, MRE requires a mechanical exciter for shear wave generation, which significantly complicates the experimental setup of the MR-guided HIFU procedure. From this perspective, Acoustic Radiation Force (ARF)-based harmonic MRE approaches have been proposed where the mechanical excitation is generated using the radiation force of the focused ultrasound itself with no need for supplementary equipment (Wu *et al* 2000, Chatelin *et al* 2016, Vappou *et al* 2018b). Yet, these harmonic MRE approaches are limited because of shear wave near-field effects, making them highly inaccurate in the central zone around the ultrasound focus.

Several transient ARF-based methods have been proposed as an alternative (Souchon *et al* 2008, Nightingale *et al* 2002, McDannold and Maier 2008, Larrat *et al* 2010, Bour *et al* 2017, de Bever *et al* 2018, Hofstetter *et al* 2019, Bercoff *et al* 2004, Liu *et al* 2015, 2017). ARF Imaging (ARFI) is a transient elastography method that was first introduced in ultrasound imaging (Nightingale *et al* 2002). MR-ARFI was initially proposed for the targeting of MR-guided HIFU, since it allows visualizing the focal spot on the image (McDannold and Maier 2008, Larrat *et al* 2010). Several studies have reported the use of the MR-ARFI displacement to monitor thermal ablations, relying on the fact that this displacement is related to the underlying tissue elasticity (Auboiroux *et al* 2012, Bour *et al* 2017, de Bever *et al* 2018). One limitation of these methods is that MR-ARFI displacement is not only related to local tissue elasticity, but also to the surrounding mechanical environment and to potential changes of tissue acoustic absorption (and hence radiation force) due to temperature. This has led to the development of shear-wave-based methods, as shear wave velocity (c) is quantitatively related to the underlying shear modulus (μ) by:

$$\mu = \rho c^2 \quad (1)$$

with ρ being the density (considered to be equal to 1000 $kg.m^{-3}$) and assuming that the biological tissue is purely linear elastic, isotropic, locally homogeneous, and incompressible (Manduca *et al* 2001). Hofstetter *et al* proposed an ARF-based method that consists in applying multiple ARF pushes at several positions to allow for composite shear modulus mapping and real-time elastography monitoring during HIFU procedures (Hofstetter *et al* 2019). An alternative method to map mechanical properties over an extended area is the Supersonic Shear wave Imaging (SSI) technique proposed by Liu *et al* (Liu *et al* 2015, 2017) based on the ultrasonic SSI method (Bercoff *et al* 2004). It consists in generating quasi-planar shear waves in the tissue with ARF and tracking their spatial propagation over time, so as to compute the shear wave velocity map from which an elastogram can be deduced. Although the MR-SSI method was shown to be particularly accurate with high field small animal preclinical setup (Liu *et al* 2015, 2017), reported acquisition times of several minutes prevent this method from being used in its current form for real-time HIFU monitoring.

The aim of this work is to develop a new HIFU ablation monitoring method capable of providing temperature and elasticity maps simultaneously and in real time, both information being derived from the same MR phase images. In the next section, we present the experimental setup and the developed algorithm for MR-SSI elastography. Then, we expose the results obtained on a calibrated phantom as well as on a gelatin phantom undergoing HIFU heating.

Methods

Focused ultrasound sequence

As introduced by Bercoff *et al*, the SSI method is based on the generation of a quasi-planar mechanical wave in the medium (Bercoff *et al* 2004). Thanks to the electronic steering abilities of the multi-element ultrasound transducer, several ARF pushes are generated successively, hence creating multiple quasi-punctual shear wave sources. When the pushes are generated at a sufficiently high speed, these waves interfere and form a quasi-planar shear wave, the propagation of which reflects the mechanical properties of the tissue. Subsequently, the HIFU heating is performed directing the focus a few millimeters away from the SSI push line (Figure 1). This set of pushes constitutes a cycle that will be repeated for each MR image acquisition (i.e., each TR) during the whole heating procedure. Once the heating completed, SSI pushes alone will be generated to maintain elasticity monitoring during the cooling down period.

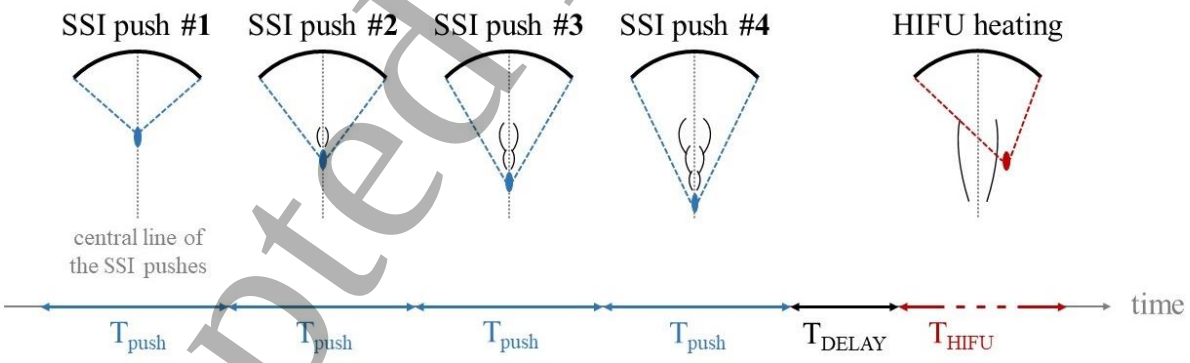

Figure 1 – Operating sequence of the focused ultrasound transducer. A quasi-planar supersonic shear wave is generated using 4 successive SSI pushes aligned on a straight line, followed by the HIFU heating located a few millimeters on the side of the SSI push line. Note that T_{HIFU} is sensitively longer than T_{push} (typically hundreds of ms vs a few ms). This time sequence is repeated in each MR image acquisition, i.e., each TR.

As the generated mechanical wave is cylindrical, the wavefronts will have different appearances depending on the orientation of the imaging plane (Figure S1 – supplementary material). When the imaging plane is parallel to the SSI push line, the shear wave appears as 2 quasi-planar wavefronts propagating in opposite directions. When the imaging plane is perpendicular to the SSI push line, a circular wavefront is observed.

MR-SSI sequence

The displacements induced by the quasi-planar shear waves are encoded with bipolar Motion-Sensitizing Gradients (MSG) added to a single-shot gradient-echo echo-planar-imaging (EPI) sequence. The bipolar MSG is synchronized with the mechanical excitation using a variable time offset Δt_{TRIG}; thus, tissue displacement is encoded at different moments of the wave propagation, below designated by "phase offsets" (Figure 2). Knowing the displacement field induced by the shear wave, the wave equation can be used to estimate the shear modulus of the underlying medium. It should be noted that for each Δt_{TRIG} value, two acquisitions are performed with opposed MSG polarities. The average between these two phase images is used for PRFS thermometry, since they bear opposite motion encoding that null each other, whereas their difference is used for shear wave reconstruction, which doubles the displacement encoding and suppresses the background phase in the phase difference image (Corbin *et al* 2016, Le *et al* 2006a, 2006b).

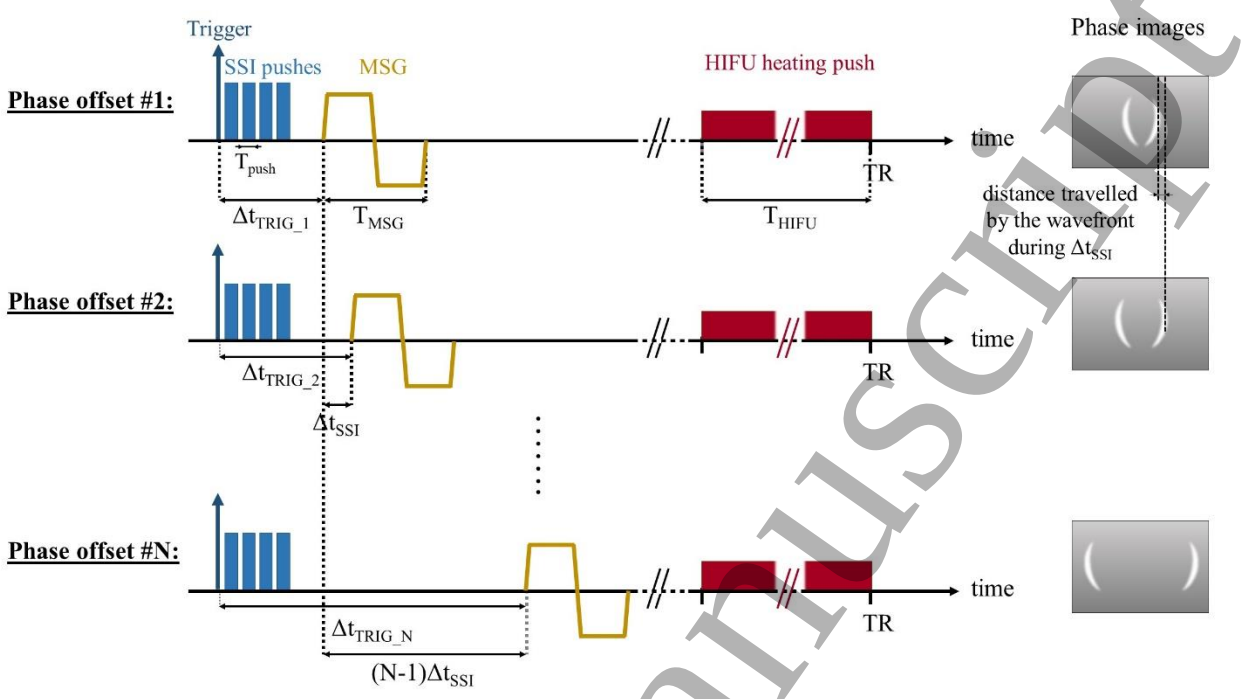

Figure 2 – Illustration of the acquired images at different SSI steps. By varying the offset Δt_{TRIG} between the SSI pushes and the encoding gradient (MSG), different phases of the propagating shear wave can be captured. Note that for simplicity, only one of the two MSG polarities has been represented. In practice, one wavefront image is obtained from the difference between two phase images acquired with the same Δt_{TRIG} but with opposed MSG polarities.

Post-processing and elastogram reconstruction

Elastograms are reconstructed using an edge detection approach followed by a time-of-flight-based method for the computation of the shear wave velocity (McCracken *et al* 2005, Liu *et al* 2017). The whole process is implemented using Matlab (The Mathworks Inc., MATLAB R2021a).

Inputs

The processing program is provided with phase difference images acquired for a set of Δt_{TRIG} values (Figure 3A). Thus, the main input of the process is a 3-dimensional matrix containing displacement images over time (2 spatial dimensions and 1 temporal dimension).

Preparation of the data and wavefront enhancement

The spatial domain is truncated to a region of interest (ROI) containing shear wavefronts. A Hessian-based multiscale filtering approach is applied to enhance the wavefronts on the images (Frangi *et al* 1998).

Shear wave velocity estimation on each line of the field of view (FOV)

To estimate the shear wave velocity, the position of each wavefront is tracked across all the propagation lines. In other words, the shear wave velocity is mapped on all the lines that are perpendicular to the wavefront. For each line, a chronogram represents the line in question over the different phase offsets sampling its propagation over time (Figure 3B). An edge detection approach (Canny filter (Canny 1986)) is implemented to delineate both edges of the wavefront (Figure 3C). These edges are referred to as "inner" and "outer" edges with respect to the SSI push line. For both edges, the arrival time of the wavefront is represented against its distance from the SSI push line. This curve is smoothed with a local regression (Figure 3D), then the local slope is estimated using a simple differential approach (Figure 3E). Finally, the shear wave velocity is locally deduced as it is inversely proportional to the previously estimated slope (Figure 3F).

Elastogram reconstruction

Depending on the imaging slice, the process will be repeated either in Cartesian or radial lines of the image. Once the shear wave velocity is estimated on all the lines of the image, we obtain two distinct maps: one using the inner edges of the wavefront and the other one using the outer edges (Figure 3G). A compound map is then reconstructed from these complementary maps, with a mean value taken on the pixels where both maps overlap (Figure 3H). The shear modulus map is deduced

using equation (1). Finally, a median filter (4×4 kernel) is applied to attenuate potential outliers (Figure 3I).

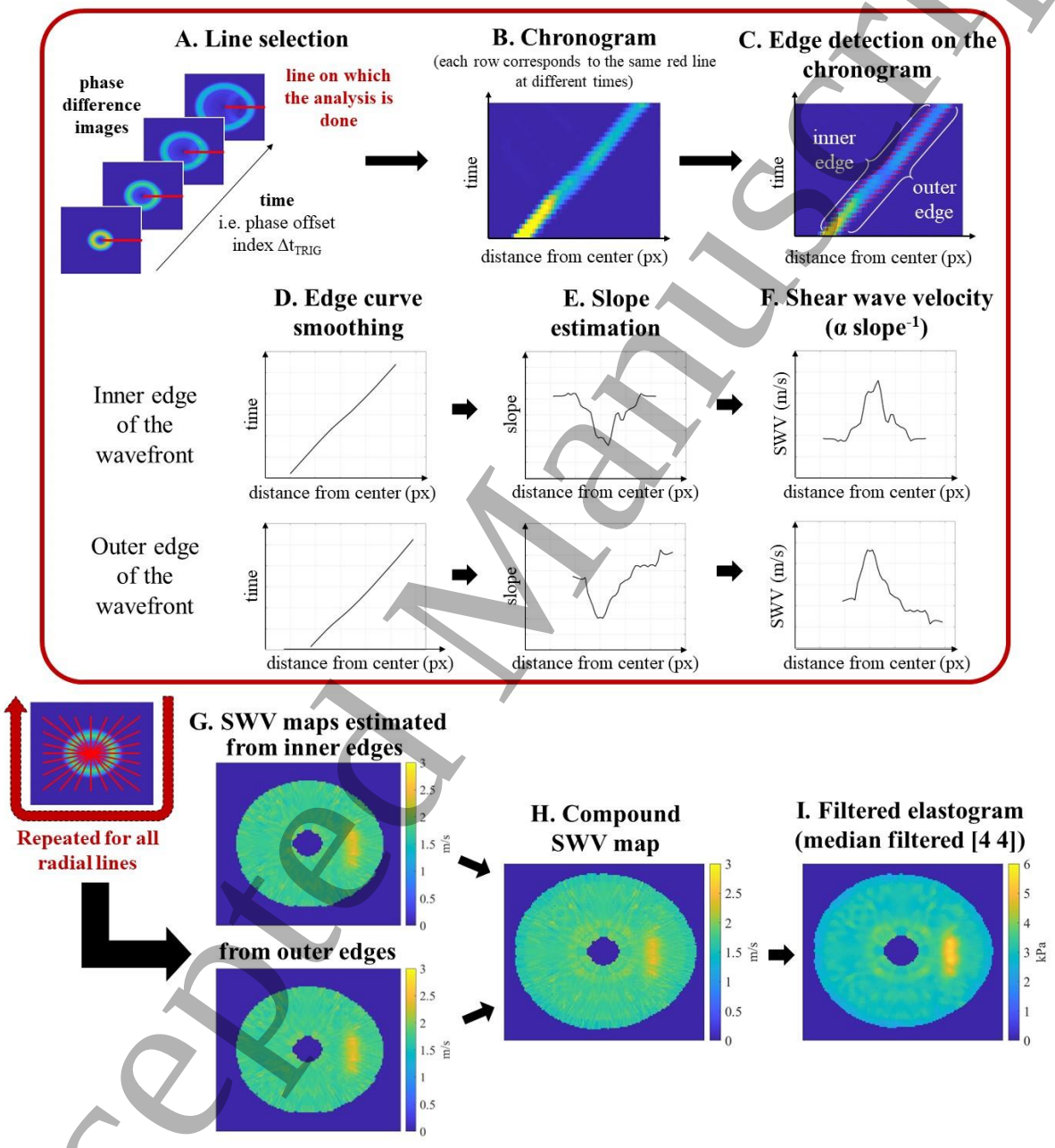

Figure 3 – MR-SSI reconstruction process. Illustration in the case of a circularly propagating SSI wavefront, i.e. the imaging plane is parallel to the SSI push line. (A) For each radial line (or Cartesian line in the case of linearly propagating SSI wavefronts, i.e., the imaging plane is perpendicular to the SSI push line), (B) a chronogram is built

showing the selected line over the different SSI steps. (C) An edge detection step allows identifying inner and outer edges of the wavefront in the chronogram, each edge representing a 1D curve. After (D) smoothing the curve, (E) a slope estimation leads to (F) the estimation of the shear wave velocity. After applying steps A-E to all the lines of the FOV, (G) two shear wave velocity (SWV) maps are obtained, one corresponding to the inner and the other one to the outer edges of the wavefronts. (H) A compound SWV map is computed from which (I) the final elastogram can be deduced. The images on this figure correspond to a simulated dataset on a 3 kPa-numerical phantom containing a 5 kPa-inclusion.

Experimental protocol

MRI acquisitions

All MR experiments were performed in a 1.5 T MRI system (MAGNETOM Aera, Siemens Healthcare, Erlangen, Germany) using a combination of Spine and 18-element body matrix coils. The single-shot gradient-echo EPI sequence was modified for real-time monitoring with MR-SSI. Relevant parameters for the acquisition were: TR/TE 500/29 ms, FOV 256 mm × 176 mm, slice thickness 5 mm, matrix 128 × 88 (80% phase lines), MSG duration 10 ms at 30 mT/m, bandwidth 1502 Hz/px, flip angle 55°, GRAPPA factor 2.

SSI experimental setup

A 128-element spherical HIFU transducer (1 MHz central frequency, 6 cm radius of curvature, 6 cm in aperture; Imasonic, Voray sur l'Ognon, France) was used to generate SSI pushes and HIFU heating (Figure 1) driven by the MR-compatible HIFU generator (Image Guided Therapy, Pessac, France). The transducer was positioned on the upper surface of the phantom with its focal axis perpendicular to the phantom surface. The acoustic coupling between the transducer and the phantom was realized using a balloon filled with degassed water, and a thin layer of degassed water over the phantom surface.

Proof-of-concept of MR-SSI in CIRS phantom

Phantom

The first experiment was realized on a commercial elastography phantom (Computerized Imaging Reference Systems, Inc. (CIRS), Norfolk, USA). The phantom contains 4 inclusions of 2 cm in diameter, having each a different shear modulus. The shear modulus values estimated with MR-SSI were compared to those provided by the manufacturer in the datasheet (obtained by static indentation), as well as to the results obtained using conventional MRE.

MR-SSI

The SSI wave was provoked by four pushes respectively at 50, 60, 70 and 78 mm from the top of the transducer active surface. Each push lasted 1.6 ms with an estimated acoustic power of 230 W.

MR-SSI images were acquired in a plane perpendicular to the SSI push line, corresponding to a coronal slice for a patient in supine position. The imaged slice was chosen to cross all 4 inclusions and, at the same time, to pass through the center of the SSI pushes (i.e., at approximately 64 mm from the top of the transducer active surface). At this point of the study, we could not determine yet the number of SSI steps necessary for the shear modulus reconstruction. Therefore, a total of 46 phase offsets were acquired with Δt_{TRIG} starting from 0 ms to 22.5 ms with increment Δt_{SSI} = 0.5 ms. The longer Δt_{TRIG} were chosen so that all 4 inclusions were covered by the propagating shear wave. Table 1 summarizes the relevant temporal parameters used in the experiments.

This experiment had three objectives: (i) to assess the ability to map the 4 inclusions of the CIRS phantom, (ii) to evaluate the repeatability of the MR-SSI process and (iii) to investigate the number of required SSI steps. For the second objective, the acquisition was repeated 8 times. As for the

last objective, we decimated the acquired dataset, and identified the minimal number of SSI steps providing similar values to those obtained with the entire dataset.

MRE

The commercial MR Elastography system (Resoundant, Rochester, MN) was set at a mechanical frequency of 150 Hz. Relevant parameters of the MRE gradient-echo sequence were: TR/TE 50/12.4 ms, FOV 300 mm × 300 mm, slice thickness 5.5 mm, matrix 128 × 128, MSG duration 6.7 ms at 28 mT/m, bandwidth 1000 Hz/px, flip angle 20°. The shear modulus was reconstructed using a Local Frequency Estimation algorithm (Knutsson *et al* 1994, Manduca *et al* 1996) under the assumption of a purely linear elastic material.

Definition of ROIs

For each inclusion, the shear modulus was averaged within an ROI defined on the magnitude image. The same process was applied to the 8 datasets acquired for MR-SSI as well as to MRE images.

Monitoring of HIFU heating in a gel phantom

Phantom

The second experiment consisted in monitoring a HIFU heating in a gelatin phantom using MR-SSI elastography and PRFS thermometry. The phantom was made of 2 kg of water, 400 g of condensed milk, and 100 g of gelatin. Before refrigeration, the mixture was degassed using a vacuum chamber.

MR-SSI

Images were acquired in a plane parallel to the SSI push line, corresponding to a transverse slice for a patient in supine position, centered at the ultrasound focus. SSI pushes were generated at depths of 42, 54, 66 and 78 mm from the top of the transducer active surface with a duration of 1.6 ms for each push and an estimated acoustic power of 230 W. The HIFU heating focus was located at a depth of 60 mm from transducer active surface (coinciding with the midpoint of the segment containing the SSI pushes) and 16 mm laterally from the SSI push line. The SSI push line and the HIFU heating focus are both contained in the chosen transverse monitoring plane. The HIFU heating shot was performed during 250 ms (duty cycle 50% compared to 1.3% for the SSI push sequence) at an estimated acoustic power of 92 W.

A pre-heating acquisition was performed to determine the phase offsets needed in order to cover the desired ROI with the spatial extent of the wave propagation. Based on the results of the first experiment and the pre-heating acquisition, a total of 10 SSI steps, ranging from Δt_{TRIG} = 1.5 ms to 15 ms with increment Δt_{SSI} = 1.5 ms (Table 1), were acquired for each SSI cycle, allowing the reconstruction of one elastogram. A temporal interpolation of factor 3 was used in the MR-SSI process.

Knowing that 2 images with opposite MSG polarities are acquired for each of the 10 SSI steps, and with a TR set to 500 ms, the elasticity map is updated every 10 s, corresponding to a refresh rate of 0.1 Hz. The refresh rate for thermometry was 1 Hz, because a thermometry map is obtained for each SSI step from averaging the 2 phase images acquired with opposed MSGs.

The HIFU heating phase lasted 120 s, followed by a cooling down phase of 120 s, in which the HIFU heating shot was not performed while SSI pushes continued to be applied so that both tissue temperature and elasticity were still measured.

Experimental data processing

Phase images were spatially unwrapped prior to SSI computations and temporally unwrapped for thermometry. B0 field drift effects in PRFS were corrected by applying phase subtraction with respect to a non-heated ROI chosen close to the HIFU heating focus.

Time (ms)	T_{push}	T_{MSG}	Δt_{TRIG_1}	Δt_{TRIG_N}	Δt_{SSI}	T_{HIFU}
Validation on CIRS (N = 46)	1.6	10	0	22.5	0.5	No heating
Monitoring on gel (N = 10)	1.6	10	1.5	15	1.5	250

Table 1 – Relevant temporal parameters of ultrasound and MRI sequences (as defined in Figure 2). Recall that N: number of SSI steps, T_{push}: duration of each of the 4 successive SSI pushes, T_{MSG}: duration of the MSG, Δt_{TRIG_1}: temporal offset between the SSI pushes and the MSG at the first SSI step, Δt_{TRIG_N}: : temporal offset between the SSI pushes and the MSG at the last SSI step, Δt_{SSI}: temporal increment between 2 successive SSI steps, T_{HIFU}: duration of the HIFU heating push.

Results

Validation on CIRS phantom

Circular wavefronts acquired with increasing phase offsets can be seen from left to right in Figure 4 with the corresponding detected edges represented in red (all images are provided in Video 1 – supplementary material). In the two phase difference images corresponding to longer phase offsets (Figure 4), one can notice that the wave propagates faster on the right side (green arrow), and slower on the left side (blue arrow). These observations are consistent with the location of the rigid and soft inclusions across the imaged slice, to the right and left side, respectively.

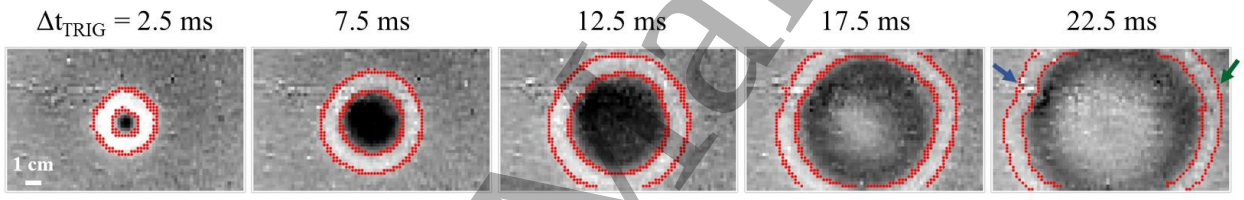

Figure 4 – Wavefronts observed at different SSI steps on the CIRS phantom. Phase difference images for increasing phase offsets (Δt_{TRIG}) between SSI push and MSG phase encoding. Red circles represent the detected inner and outer edges of the wavefronts. Arrows on the last frame show the regions where the wave propagated faster (green) and slower (blue) due to the presence of inclusions with different shear moduli.

By applying the SSI reconstruction process, we obtained the shear modulus map presented in Figure 5A (obtained with one of the 8 acquired datasets). Mean shear moduli in each ROI are given in Table 2 in kPa with standard deviations as percentages. Note that the values shown for MR-SSI represent the average of the 8 datasets (at each cell, are given the average of the 8 obtained shear moduli and the average of the 8 standard deviations).

The MR-SSI computed shear modulus of the background was 6.1 kPa (compared to 5.9 kPa from the datasheet). For inclusions I-IV, the shear moduli were measured to 4.5, 4.8, 7.3 and 11.5 kPa

respectively. In comparison with the CIRS datasheet, MR-SSI provided higher values for soft inclusions (types I and II) and lower values for rigid ones (types III and IV). A better consistency was found between SSI and MRE results, with a maximum difference of 1.3 kPa between these two methods. In terms of homogeneity, the shear moduli estimated with MR-SSI have standard deviations of 15%, 12%, 22%, 22% and 17% for inclusions I-IV and the background respectively.

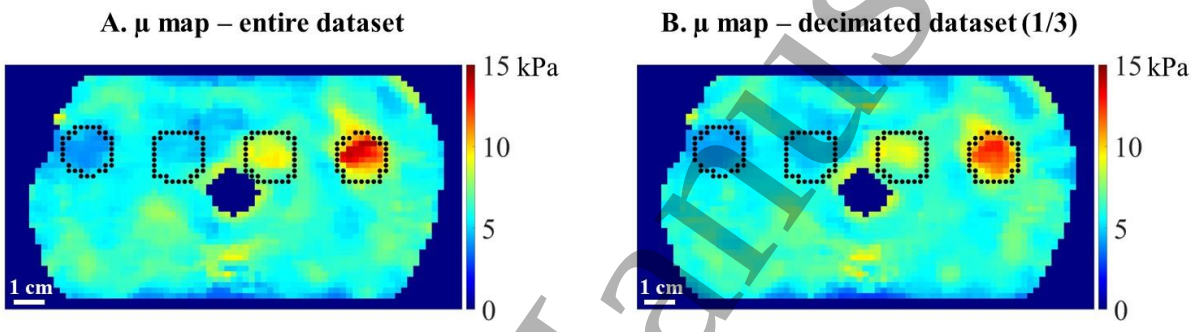

Figure 5 – Shear modulus maps obtained on the CIRS phantom. (A) using the entire dataset and (B) the decimated dataset (decimation 1/3 then interpolation ×3). Black circles represent the selected ROIs in the inclusions. Inclusions are referred to as type I, II, III and IV (from left to right) by the manufacturer.

Shear modulus (kPa)	**Type I**	**Type II**	**Type III**	**Type IV**	**Background**
CIRS datasheet	1.9	3.4	11.6	23.8	5.9
MRE (150 Hz)	3.6 ± 23%	3.7 ± 11%	7.5 ± 7%	10.2 ± 13%	6.1 ± 15%
MR-SSI (entire dataset)	4.5 ± 15%	4.8 ± 12%	7.3 ± 22%	11.5 ± 22%	6.1 ± 17%
MR-SSI (decimation 1/3 then interpolation ×3)	4.5 ± 17%	4.8 ± 12%	7.2 ± 22%	11.6 ± 23%	6.1 ± 19%

Table 2 – Shear moduli for the 4 inclusions and the background of the CIRS phantom, obtained from the datasheet, MRE 150 Hz, MR-SSI with the entire datasets (phase offset 0 to 22.5 ms with 0.5 ms step) and MR-SSI with the decimated datasets (1/3 followed by interpolation ×3). Note that the values shown for MR-SSI correspond to the average of the 8 datasets ± the average of the 8 standard deviations in the ROI.

Figure 6 represents the boxplots obtained from the 8 shear modulus maps acquired on the CIRS phantom (using the full datasets i.e., without decimation). The standard deviations between the 8 results are of 4%, 9%, 6%, 11% and 2% for inclusions I-IV and the background respectively which shows the high repeatability of our process.

In order to increase the temporal resolution of MR-SSI for real-time monitoring, we tested whether the number of SSI steps could be reduced while maintaining sufficient information. It was found that with a decimation of factor 3 (i.e. keeping 1 out of each 3 SSI steps) followed by an interpolation of the same factor (to compensate the missing phase offsets), the elasticity map (Figure 5B) and the mean shear moduli (Table 2, last line) remained close to those obtained with the full dataset. The maximum difference between the two datasets is equal to 0.1 kPa. Δt_{SSI} was therefore set to 1.5 ms (3×0.5 ms) for the monitoring experiment.

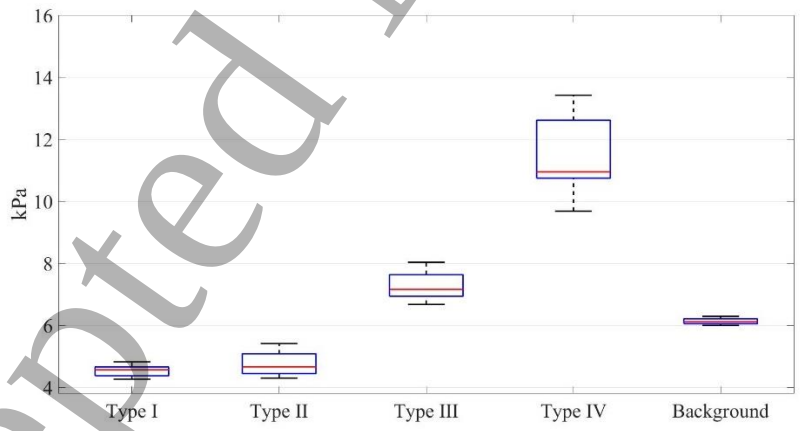

Figure 6 – Boxplot of the shear moduli obtained with the MR-SSI process in the CIRS phantom (8 datasets)

Monitoring of HIFU heating in a gel phantom

Figure 7 presents the SSI wavefronts before and at the end of the HIFU heating. It can be noticed that at the end of the heating, the wavefront on the right side did not go as far as it had gone before

the heating (red vertical line in Figure 7) suggesting that planar shear waves slow down over time (Video 2 – supplementary material). This decrease of the shear wave velocity was expected because the gel softens during heating. This is consistent with the elasticity maps obtained with MR-SSI where the shear modulus is found to decrease on the right side, at the same position where the temperature increased during the HIFU heating (Video 3 – supplementary material).

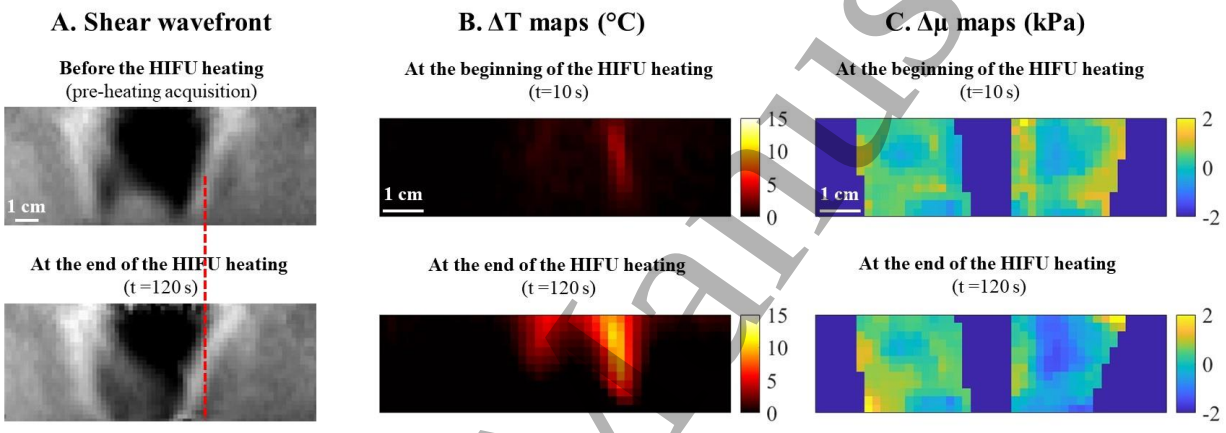

Figure 7 – Shear wavefront, thermometry and elastography maps before and after the HIFU heating. (A) The red dotted line indicates the inner edge of the right-side wavefront at the beginning of the heating. At t = 120 s, the wavefront on the right side is slowed down, suggesting local gel softening as a result of the HIFU heating. Temperature increase and shear modulus decrease occurring on the heating side can be seen on ΔT (B) and Δμ (C) maps.

Figure 8 presents elasticity and temperature changes averaged within a 5×3-pixel ROI selected around the heating focus on the thermometry map. As expected, temperature and shear modulus remained nearly constant during the whole experiment on the left side (symmetrical ROI with regards to the SSI push line). As for the right side, the temperature increase ΔT reached 9 °C while the shear modulus μ decreased from 2.9 kPa ± 5% to 1.8 kPa ± 17% between the beginning and

the end of the heating. While the temperature started decreasing once the HIFU heating stopped, the shear modulus remained steady at 1.8 kPa during the following 120 s.

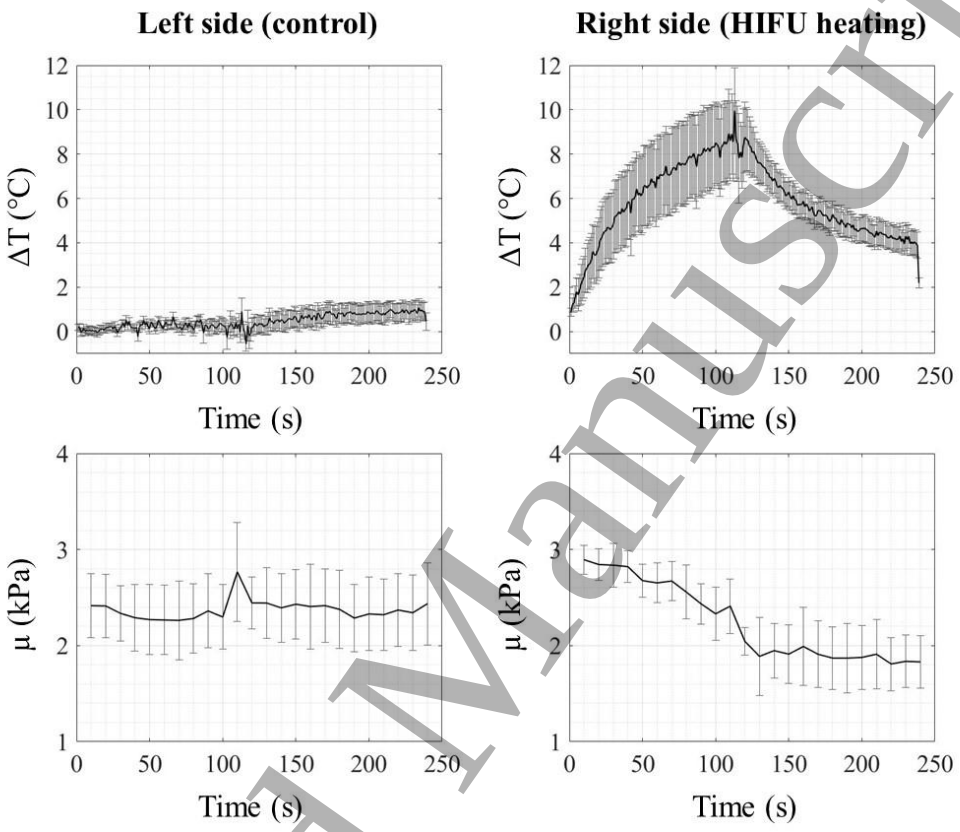

Figure 8 – Changes in temperature and shear modulus averaged within a 5×3-pixel ROI on the left side (control) and on the right side (HIFU heating) of the SSI push line. Error bars represent the standard deviation of temperature over the selected ROI. On the right-side, heating the gelatin results in significant softening, whereas no significant changes are observed on the left side (control).

Discussion

In this paper, an MRI protocol and a reconstruction process have been proposed for the MR-SSI elastography method for the monitoring of elasticity and temperature changes during HIFU ablation. The proposed reconstruction process relies on two main steps: (i) shear wavefront tracking using an edge detection approach and (ii) shear wave velocity mapping based on a time-of-flight method. This elastography technique was first validated on a calibrated phantom where inclusions with different shear moduli could be mapped with high repeatability. Second, the HIFU heating experiment emphasized the ability to map in real time the irreversible elasticity changes caused by HIFU in a gel phantom. The shear modulus decrease at the heating focus was monitored on elasticity maps refreshed every 10 s. The shear modulus remained steady during the whole cooling down phase, which emphasizes the relevance of mechanical properties as biomarkers of thermal damage.

As presented previously, our MR-SSI elastogram reconstruction process is based on a time-of-flight computation, a principle also proposed by McCracken *et al* and Liu *et al* (McCracken *et al* 2005, Liu *et al* 2017) for shear wave velocity estimation. However, instead of extracting the maximum peak on the wave profiles, we chose to detect both the inner and outer edges of the wavefront. By doing so, the information is duplicated and 2 distinct elastograms can be obtained which allows averaging the shear modulus on the area where both maps overlap and so, reduce the number of potential outliers in this region.

Several limitations of the proposed method need to be highlighted. First, elasticity estimation may be subject to significant averaging effects. This is mainly explained by the fact that spatial resolution of the SSI elastograms is entirely dependent on the temporal resolution of SSI images.

In other words, the more SSI steps are acquired, the better the resolution of the computed elasticity maps is. However, the number of SSI steps should be maintained reasonably low to ensure a high temporal update rate of elasticity. Thus, it is necessary to find an acceptable compromise between temporal and spatial resolutions of the estimated elastograms. In addition, operations such as interpolation and smoothing have supplementary averaging effects on the final elasticity values. Second, several phenomena may limit the spatial coverage and the accuracy of the obtained elastograms. As for spatial coverage, elasticity cannot be mapped neither near the SSI push line because of shear wave near-field effects, nor too far from this same line because of wave attenuation, which makes the wavefront detection more difficult. As for accuracy, guided wave phenomena can lead to inaccuracy of shear wave velocity estimates at interfaces between media with different mechanical properties. These limitations could justify the differences between the MR-SSI results and the values provided in the CIRS datasheet. Indeed, the previously mentioned averaging effects may partially explain why the shear moduli obtained for the inclusions softer than the background were higher than expected, and inversely for the rigid inclusions. It is also important to note that elasticity values reported by the manufacturer have been obtained by mechanical indentation, a static mechanical testing method that could also account for some of the observed differences. All these reasons may explain the better consistency between MR-SSI and conventional MRE as they are both dynamic elastography approaches, based on shear wave propagation. This was further highlighted by the repeatability study performed on the CIRS which shows that MR-SSI and MRE results are in good agreement. Although its accuracy needs to be further evaluated, particularly in heterogeneous media for the aforementioned reasons, MR-SSI was shown to be a repeatable method providing a quantitative biomarker of structural damage induced by heating.

A key parameter of the SSI method is the temporal step Δt_{SSI} that must be determined with attention. Indeed, the higher the rigidity of the tissue, the smaller the Δt_{SSI} should be to ensure a sufficient temporal resolution within an SSI cycle. Therefore, preliminary acquisitions are required to obtain an estimation of the expected tissue elasticity, since this will influence the value of the SSI step Δt_{SSI} that will be chosen. In practice, a pre-ablation MR-SSI acquisition may be performed so the user can estimate the range and number of SSI phase offsets that will provide adequate spatial coverage of the propagating wave for the following monitoring acquisitions. The results presented in this paper are limited since they do not include in vitro or in vivo tissues. Therefore, further investigation is necessary to find the optimal range of SSI phase offsets as well as the Δt_{SSI} step as they will depend on the elasticity of the tissue as well as its heterogeneities.

In vitro or in vivo tissue experiments would allow reaching much higher temperatures such as those used clinically during HIFU ablations. Gelatin is not a suitable model for high temperature experiments as it melts, thus preventing the generation and propagation of shear waves. In practice, higher temperatures can be achieved by increasing the acoustic power of the HIFU heating push (which was set at only 40% of the maximal power of the transducer for the heating experiment on gelatin) and/or its duty cycle (set to 50% here). It should be noted that higher duty cycles can be achieved for the HIFU heating push. This duty cycle could be further increased through the use of a real-time industrial version of the communication software between the HIFU generator and the MRI console, or through the use of longer TR, though at the expense of the SSI temporal resolution.

Several approaches have already been proposed for MR-guided HIFU monitoring using the mechanical properties of the tissue. As opposed to MRE, MR-SSI does not require an additional mechanical exciter since the ARF is used to generate the pushes. Nonetheless, a potential risk of

this method could be to induce some thermal effects along the SSI push line. This is mainly avoided by the short duration as well as the low duty cycle of the pushes. The mild heating observed along the SSI push line in the second experiment (+6 °C maximum) does not entail any change in the phantom structure, and it is deemed to be lower in a perfused organ. Furthermore, this heating along the SSI push line was mainly observed in experiments where a HIFU heating was performed simultaneously with the MR-SSI elastography measurements. No significant heating was observed in MR-SSI experiments without HIFU heating phase. This could be explained by the fact that the HIFU wave delivers a certain amount of energy along the whole ultrasound cone. Although this energy is mostly absorbed at the focus, the summation of energy on the areas where several ultrasound cones are superimposed may induce a mild temperature increase (especially in the presence of a long HIFU heating push, and in the absence of perfusion). This is visible in Video 3, as mild heating occurs along the SSI push line only during the HIFU heating phase, followed by a plateau during the cooling down phase despite the fact that the SSI pushes were still generated. When comparing to other ARF-based approaches, MR-SSI is distinguished by its ability to provide an extended spatial mapping of elasticity whereas other methods such as MR-ARFI estimate a single value at the focus (Vappou *et al* 2018). The method proposed by Hofstetter *et al* (Hofstetter *et al* 2019) also allows for spatial elasticity mapping. It relies on the generation of multiple pushes in a plane perpendicular to the ultrasound propagation axis, allowing reconstructing elasticity maps every 12 seconds. Our method instead relies on the generation of quasi-cylindrical supersonic shear waves, which, in theory, are more contrasted and less attenuated than spherical waves. This may explain the larger spatial extent of our MR-SSI method in a coronal slice (a circular field of view of about 13 cm in diameter on the CIRS phantom) compared to the method of Hofstetter *et al* where elasticity has been measured on a circular field of view of 5 cm in diameter. Another

relevant point of comparison is the applicability of our MR-SSI method in different imaging planes as the composite shear wave used by Hofstetter *et al* makes the method only applicable in coronal slices. Nonetheless, this latter was also demonstrated in 3D providing elasticity measurements over several slices with an acquisition time of 144 seconds. Finally, both approaches allow mapping elasticity in 2D with similar refresh rates compatible with real-time monitoring.

Being equivalently applicable in different imaging planes adds a supplementary degree of freedom to MR-SSI. A transverse imaging slice has been chosen for the HIFU heating experiment as the HIFU focus has an ellipsoidal shape of about 1 cm in length and 1-2 mm in diameter. Thus, mapping the elasticity in a transverse plane is much more relevant in order to detect the variations along the length of the ellipsoidal lesion. Therefore, the possibility to choose the imaging plane according to the shape and size of the expected tissue heterogeneities is an advantage of the proposed method.

Although theoretically, the MR-SSI method can be used with non-EPI sequences, the need for high temporal resolution virtually imposes the use of single-shot EPI acquisitions, with all related artifacts and limitations. Single-shot EPI with longer TR also offers optimal duty cycle balance between the expected low duty cycle at the SSI push line (limited heating), and the high duty cycle necessary at the HIFU ablation spot.

Conclusion

The proposed MR-SSI method allows simultaneous temperature and elasticity mapping. This method was first evaluated on a heterogeneous phantom and was then used for the monitoring of HIFU ablations, with MR-SSI elastograms updated every 10 seconds and relative temperature maps updated every second. In the case of a gelatin phantom, the shear modulus was found to decrease during the HIFU heating, thus reflecting that MR-SSI can be a promising technique to assess the structural changes of tissue during a HIFU treatment.

Acknowledgements

This work has benefitted from funding of the FUI (Fonds Unique Interministériel, BPI France) for the UFOGUIDE project, and the ANR (Agence Nationale de la Recherche) French national program “Investissements d’Avenir” for the LABEX-CAMI (ANR-11-LABX-004) and the TechnoFUS joint laboratory project (ANR-21-LCV3-0007-01), and the IHU Strasbourg (Institute of Image Guided Surgery, ANR-10-IAHU-02).

References

Arnal B, Pernot M and Tanter M 2011 Monitoring of thermal therapy based on shear modulus changes: II. Shear wave imaging of thermal lesions *IEEE Trans. Ultrason., Ferroelect., Freq. Contr.* **58** 1603–11

Auboiroux V, Viallon M, Roland J, Hyacinthe J-N, Petrusca L, Morel D R, Goget T, Terraz S, Gross P, Becker C D and Salomir R 2012 ARFI-prepared MRgHIFU in liver: Simultaneous mapping of ARFI-displacement and temperature elevation, using a fast GRE-EPI sequence *Magnetic Resonance in Medicine* **68** 932–46

Bercoff J, Tanter M and Fink M 2004 Supersonic shear imaging: a new technique for soft tissue elasticity mapping *IEEE Trans. Ultrason., Ferroelect., Freq. Contr.* **51** 396–409

de Bever J T, Odéen H, Hofstetter L W and Parker D L 2018 Simultaneous MR thermometry and acoustic radiation force imaging using interleaved acquisition: Simultaneous MR Thermometry and ARFI *Magn. Reson. Med.* **79** 1515–24

Bour P, Marquet F, Ozenne V, Toupin S, Dumont E, Aubry J-F, Lepetit-Coiffe M and Quesson B 2017 Real-time monitoring of tissue displacement and temperature changes during MR-guided high intensity focused ultrasound: Monitoring of Changes During MRgHIFU *Magn. Reson. Med* **78** 1911–21

Canny J 1986 A Computational Approach to Edge Detection *IEEE Trans. Pattern Anal. Mach. Intell.* **PAMI-8** 679–98

Chatelin S, Charpentier I, Corbin N, Meylheuc L and Vappou J 2016 An automatic differentiation-based gradient method for inversion of the shear wave equation in magnetic resonance elastography: specific application in fibrous soft tissues *Phys. Med. Biol.* **61** 5000–19

Chen J, Woodrum D A, Glaser K J, Murphy M C, Gorny K and Ehman R 2014 Assessment of in vivo laser ablation using MR elastography with an inertial driver: Laser Ablation MRE with Inertial Driver *Magn. Reson. Med.* **72** 59–67

Corbin N, Vappou J, Breton E, Boehler Q, Barbé L, Renaud P and Mathelin M 2016 Interventional MR elastography for MRI-guided percutaneous procedures *Magn. Reson. Med.* **75** 1110–8

E. Konofagou E, Maleke C and Vappou J 2012 Harmonic Motion Imaging (HMI) for Tumor Imaging and Treatment Monitoring *CMIR* **8** 16–26

Frangi A F, Niessen W J, Vincken K L and Viergever M A 1998 Multiscale vessel enhancement filtering *Medical Image Computing and Computer-Assisted Intervention — MICCAI'98* Lecture Notes in Computer Science vol 1496, ed W M Wells, A Colchester and S Delp (Berlin, Heidelberg: Springer Berlin Heidelberg) pp 130–7 Online: http://link.springer.com/10.1007/BFb0056195

Geoghegan R, ter Haar G, Nightingale K, Marks L and Natarajan S 2022 Methods of monitoring thermal ablation of soft tissue tumors – A comprehensive review *Medical Physics* mp.15439

Hofstetter L W, Odéen H, Bolster B D, Mueller A, Christensen D A, Payne A and Parker D L 2019 Efficient shear wave elastography using transient acoustic radiation force excitations and MR displacement encoding *Magn Reson Med* **81** 3153–67

Ishihara Y, Calderon A, Watanabe H, Okamoto K, Suzuki Y, Kuroda K and Suzuki Y 1995 A precise and fast temperature mapping using water proton chemical shift *Magn. Reson. Med.* **34** 814–23

Knutsson H, Westin C-F and Granlund G 1994 Local multiscale frequency and bandwidth estimation *Proceedings of 1st International Conference on Image Processing* Proceedings of 1st International Conference on Image Processing vol 1 pp 36–40 vol.1

Larrat B, Pernot M, Aubry J-F, Dervishi E, Sinkus R, Seilhean D, Marie Y, Boch A-L, Fink M and Tanter M 2010 MR-guided transcranial brain HIFU in small animal models *Phys. Med. Biol.* **55** 365–88

Le Y, Glaser K, Rouviere O, Ehman R and Felmlee J P 2006a Feasibility of simultaneous temperature and tissue stiffness detection by MRE *Magn. Reson. Med.* **55** 700–5

Le Y, Primak S V, Glaser K J, Manduca A, Ehman R L and Felmlee J P 2006b Simultaneous Monitoring of MRgFUS Temperature and Tissue Stiffness in Real Time *Proc. Intl. Soc. Mag. Reson. Med.* 1431

Lewa C J 1991 Magnetic Resonance Imaging in the Presence of Mechanical Waves *Spectroscopy Letters* **24** 55–67

Liu Y, Fite B Z, Mahakian L M, Johnson S M, Larrat B, Dumont E and Ferrara K W 2015 Concurrent Visualization of Acoustic Radiation Force Displacement and Shear Wave Propagation with 7T MRI ed A A Oberai *PLoS ONE* **10** e0139667

Liu Y, Liu J, Fite B Z, Foiret J, Ilovitsh A, Leach J K, Dumont E, Caskey C F and Ferrara K W 2017 Supersonic transient magnetic resonance elastography for quantitative assessment of tissue elasticity *Physics in Medicine & Biology* **62** 4083

Manduca A, Muthupillai R, Rossman P J, Greenleaf J F and Ehman R L 1996 Local wavelength estimation for magnetic resonance elastography *Proceedings of 3rd IEEE International Conference on Image Processing* Proceedings of 3rd IEEE International Conference on Image Processing vol 3 pp 527–30 vol.3

Manduca A, Oliphant T E, Dresner M A, Mahowald J L, Kruse S A, Amromin E, Felmlee J P, Greenleaf J F and Ehman R L 2001 Magnetic resonance elastography: Non-invasive mapping of tissue elasticity *Medical Image Analysis* **5** 237–54

Mariani A, Kwiecinski W, Pernot M, Balvay D, Tanter M, Clement O, Cuenod C A and Zinzindohoue F 2014 Real time shear waves elastography monitoring of thermal ablation: in vivo evaluation in pig livers *Journal of Surgical Research* **188** 37–43

McCracken P J, Manduca A, Felmlee J and Ehman R L 2005 Mechanical transient-based magnetic resonance elastography *Magnetic Resonance in Medicine* **53** 628–39

McDannold N and Maier S E 2008 Magnetic resonance acoustic radiation force imaging: Magnetic resonance acoustic radiation force imaging *Med. Phys.* **35** 3748–58

Muthupillai R, Rossman P J, Lomas D J, Greenleaf J F, Riederer S J and Ehman R L 1996 Magnetic resonance imaging of transverse acoustic strain waves *Magn. Reson. Med.* **36** 266–74

Nightingale K, Soo M S, Nightingale R and Trahey G 2002 Acoustic radiation force impulse imaging: in vivo demonstration of clinical feasibility *Ultrasound in Medicine & Biology* **28** 227–35

Odéen H and Parker D L 2019 Magnetic resonance thermometry and its biological applications – Physical principles and practical considerations *Progress in Nuclear Magnetic Resonance Spectroscopy* **110** 34–61

Quesson B, de Zwart J A and Moonen C T W 2000 Magnetic resonance temperature imaging for guidance of thermotherapy *J. Magn. Reson. Imaging* **12** 525–33

Rieke V and Butts Pauly K 2008 MR thermometry *J. Magn. Reson. Imaging* **27** 376–90

Sapareto S A and Dewey W C 1984 Thermal dose determination in cancer therapy *International Journal of Radiation Oncology*Biology*Physics* **10** 787–800

Sapin-de Brosses E, Gennisson J-L, Pernot M, Fink M and Tanter M 2010 Temperature dependence of the shear modulus of soft tissues assessed by ultrasound *Phys. Med. Biol.* **55** 1701–18

Souchon R, Salomir R, Beuf O, Milot L, Grenier D, Lyonnet D, Chapelon J-Y and Rouvière O 2008 Transient MR elastography (t-MRE) using ultrasound radiation force: Theory, safety, and initial experiments in vitro *Magn. Reson. Med.* **60** 871–81

Vappou J, Bour P, Marquet F, Ozenne V and Quesson B 2018 MR-ARFI-based method for the quantitative measurement of tissue elasticity: application for monitoring HIFU therapy *Phys. Med. Biol.* **63** 095018

Vappou J, Cabras P, Kim K, Rao P, Gangi A and Breton E 2018b Monitoring High Intensity Focused Ultrasound (HIFU) ablations in real time using interventional MR Elastography (MRE) *Proc. Intl. Soc. Mag. Reson. Med.*

Wu T, Felmlee J P, Greenleaf J F, Riederer S J and Ehman R L 2001 Assessment of thermal tissue ablation with MR elastography *Magn. Reson. Med.* **45** 80–7

Wu T, Felmlee J P, Greenleaf J F, Riederer S J and Ehman R L 2000 MR imaging of shear waves generated by focused ultrasound *Magnetic Resonance in Medicine* **43** 111–5

Yuan L, Glaser K J, Rouviere O, Gorny K R, Chen S, Manduca A, Ehman R L and Felmlee J P 2007 Preliminary assessment of one-dimensional MR elastography for use in monitoring focused ultrasound therapy *Phys. Med. Biol.* **52** 5909–19